Topological Features in Vector Fields

Thomas Wischgoll and Joerg Meyer

Electrical Engineering and Computer Science, University of California, Irvine
[twischgo|jmeyer]@uci.edu

Summary. Vector fields occur in many application domains in science and engineering. In combustion processes, for instance, vector fields describe the flow of gases. This process can be enhanced using vector field visualization techniques. Also, wind tunnel experiments can be analyzed. An example is the design of an air wing. The wing can be optimized to create a smoother flow around it. Vector field visualization methods help the engineer to detect critical features of the flow. Consequently, feature detection methods gained great importance during the last years.

Methods based on topological features are often used to visualize vector fields because they clearly depict the structure of the vector field. Most algorithms basically focus on singularities as topological features. But singularities are not the only features that typically occur in vector fields. To integrate other features as well, this paper defines a topological feature for vector fields based upon the asymptotic behavior of the flow. This article discusses techniques that are able to detect this feature.

Key words: Topological analysis, Vector field visualization, Flow visualization, Closed streamlines, Feature detection.

1 Introduction

Many of the problems in natural science and engineering involve vector fields. Fluid flows, electric and magnetic fields are nearly everywhere, therefore measurements and simulations of vector fields are increasing dramatically. As with other data, analysis is much slower and still needs improvement. Mathematical methods together with visualization can provide help in this situation. In most cases, the scientist or engineer is interested in integral curves of the vector field such as streamlines in fluid flows or magnetic field lines. The qualitative nature of these curves can be studied with topological methods developed originally for dynamical systems. Especially in the area of fluid mechanics, topological analysis and visualization have been used successfully [9, 13, 18, 25].

But often, topological methods cover only a few topological features that can occur in vector fields. Basically, only the singularities of a flow are considered in most algorithms. For instance, a sink is not the only topological feature that is able to attract the surrounding flow. This becomes quite evident when thinking about bifurcation. Consider the Hopf bifurcation as an

example. There, a closed streamline may arise from a sink. This closed streamline then has the same properties as the sink it originated from: it attracts the flow in exactly the same way. Based on this motivation, this paper defines a general topological feature that covers singularities such as sources and sinks but also other features depending on their attracting or repelling property.

First, an introduction of existing vector field visualization methods is given including topological techniques. Then, topological features are discussed and a clear definition of a topological feature based on asymptotic behavior of the flow is given. Subsequently, algorithms are described that are able to detect this kind of feature. Finally, results are shown and future work is discussed.

2 Related Works

Several visualization methods for vector fields are available at present. Here, the focus is on describing those methods that are useful in this application area. An overview over the various visualization methods can also be found in other publications [10] and PhD theses [19, 26].

Topological methods depict the structure of the flow by connecting sources, sinks, and saddle singularities with separatrices. Critical points were first investigated by Perry [22], Dallmann [5], Chong [4] and others. The method itself was first introduced in visualization for two-dimensional flows by Helman and Hesselink [12]. Several extensions to this method exist. Scheuermann et al [25] extended this method to work on a bounded region. To get the whole topological skeleton of the vector field, points on the boundary have to be taken into account also. These points are called boundary saddles. To create a time dependent topology for two-dimensional vector fields, Helman and Hesselink [13] use the third coordinate to represent time. This results in surfaces representing the evolution of the separatrices. A similar method is proposed by Tricoche et al. [27, 28] but this work focuses on tracking singularities through time. Although closed streamlines can act in the same way as sources or sinks, they are ignored in the considerations of Helman and Hesselink and others.

To extend this method to three-dimensional vector fields, Globus et al. [9] present a software system that is able to extract and visualize some topological aspects of three-dimensional vector fields. The various critical points are characterized using the eigenvalues of the Jacobian. This technique was also suggested by Helman and Hesselink [13]. But the whole topology of a three-dimensional flow is not yet available. There, stream-surfaces are required to represent separatrices. A few algorithms for computing stream-surfaces exist [16, 24] but are not yet integrated in a topological algorithm.

There are a few algorithms that are capable of finding closed streamlines in dynamical systems that can be found in the numerical literature. Aprille and Trick [2] propose a so called shooting method. There, the fixed point of the Poincaré map is found using a numerical algorithm like Newton-Raphson. Dellnitz et al. [7] detect almost cyclic behavior. It is a stochastic approach where the Frobenius-Perron operator is discretized. This stochastic measure identifies regions where trajectories stay very long. But these mathematical methods typically depend on continuous dynamical systems where a closed form description of the vector field is available. This is usually not the case in visualization and simulation where the data is given on a grid and interpolated

inside the cells. Van Veldhuizen [29] uses the Poincaré map to create a series of polygons approximating an attracting closed streamline. The algorithm starts with a rough approximation of the closed streamline. Every vertex is mapped by the Poincaré map iteratively to get a finer approximation. Then, this series converges to the closed streamline. De Leeuw et al. [6] present a simplification method based on the Poincaré index to simplify two-dimensional vector fields. An example is shown where a closed streamline is simplified to a single critical point. Even though the method might be able to detect closed streamlines in a two-dimensional flow based on the Poincaré index, it is hardly extendable to 3-D.

To get a hierarchical approach for the visualization of invariant sets, and therefore of closed streamlines as well, Bürkle et al. [3] enclose the invariant set by a set of boxes. They start with a box that surrounds the invariant set completely which then is successively bisected in cycling directions. The publication of Guckenheimer [11] gives a detailed overview concerning invariant sets in dynamical systems.

Some publications deal with the analysis of the behavior of dynamical systems. Schematic drawings showing the various kinds of closed streamlines can be found in the books of Abraham and Shaw [1]. Fischel et al. [8] presented a case study where they applied different visualization methods to dynamical systems. In their applications also strange attractors, such as the Lorentz attractor, and closed streamlines occur.

Wegenkittl et al. [30] visualize higher dimensional dynamical systems. To display trajectories, parallel coordinates [17] are used. A trajectory is sampled at various points in time. Then, these points are displayed in the parallel coordinate system and a surface is extruded to connect these points. Hepting et al. [14] study invariant tori in four dimensional dynamical systems by using suitable projections into three dimensions to enable detailed visual analysis of the tori.

Löffelmann [19, 20] uses Poincaré sections to visualize closed streamlines and strange attractors. Poincaré sections define a discrete dynamical system of lower dimension which is easier to understand. The Poincaré section which is transverse to the closed streamline is visualized as a disk. On the disk, spot noise is used to depict the vector field projected onto that disk. Using this method, it can be clearly recognized whether the flow, for instance, spirals around the closed streamline and is attracted or repelled or if it is a rotating saddle. Additionally, streamlines and stream-surfaces show the vector field in the vicinity of the closed streamline.

3 Theory

This chapter introduces the fundamental theory which is needed for the following sections. The description mainly follows the book of Hirsch and Smale [15].

3.1 Data Structures

In most applications in scientific visualization the data is not given as a closed form solution. The same holds for vector fields. Often, a vector field results

from a simulation or an experiment where the vectors are measured. In such a case, the vectors are given at only some points of the domain of the Euclidean space. These points are then connected by a grid. A special interpolation computes the vectors inside each cell of that grid. In this paper, we restrict ourselves to a few types of grids, basically triangular and tetrahedral grids. Using barycentric coordinates, vectors inside the cells can be interpolated linearly from the vectors given at the vertices [26, 31].

3.2 Vector Field Features

From a topological point of view critical points are an important part of vector fields. This special feature is described in more detail in this section. We start with the definition of critical points in the general case and then classify different types of singularities.

Definition 3.1 (Critical point)
Let $v : W \to \mathbb{R}^n$ be a vector field which is continuously differentiable. Let further $x_0 \in W$ be a point where $v(x) = 0$. Then x_0 is called a ***critical point****,* ***singularity****,* ***singular point****,* ***zero****, or* ***equilibrium*** *of the vector field.*

Critical points can be classified using the eigenvalues of the derivation of the vector field. For instance, we can identify *sinks* that purely attract the flow in the vicinity while *sources* repel it purely. A proof for this attracting respectively repelling behavior can be found in [15].

Definition 3.2 (Sink and Source)
Let v be a vector field which is continuously differentiable and x_0 a critical point of v. Let further $Dv(x_0)$ be the derivation of the vector field v at x_0. If all eigenvalues of $Dv(x_0)$ have negative real parts, x_0 is called a ***sink****. If all eigenvalues of $Dv(x_0)$ have positive real parts, x_0 is called a* ***source****.*

Streamlines are a very intuitive way to depict the behavior of the flow. But when computing such a streamline it may occur that the streamline computation does not terminate. This mostly is due to closed streamlines where the streamline ends up in a loop that cannot be left. These closed streamlines are introduced and explained in this section. More about the theoretical background can be found in several books [34, 23].

Definition 3.3 (Closed streamline)
Let v be a vector field. A ***closed streamline*** *$\gamma : \mathbb{R} \to \mathbb{R}^n, t \mapsto \gamma(t)$ is a streamline of a vector field v such that there is a $t_0 \in \mathbb{R}$ with $\gamma(t + nt_0) = \gamma(t)$ $\forall n \in \mathbb{N}$ and γ not constant.*

3.3 General Features in Vector Fields

The topological analysis of vector fields considers the asymptotic behavior of streamlines. To describe this asymptotic behavior we have two different kinds of so called limit sets, the origin set or α-limit set of a streamline and the end set or ω-limit set.

Definition 3.4 (α- and ω-limit set)
Let s be a streamline in a given vector field v. Then we define the ***α-limit*** *set as the following set: $\{p \in \mathbb{R}^n | \exists (t_n)_{n=0}^{\infty} \subset \mathbb{R}, t_n \rightarrow -\infty, \lim_{n\rightarrow\infty} s(t_n) \rightarrow p\}$, while the* ***$\omega$-limit*** *set is defined as follows: $\{p \in \mathbb{R}^n | \exists (t_n)_{n=0}^{\infty} \subset \mathbb{R}, t_n \rightarrow \infty, \lim_{n\rightarrow\infty} s(t_n) \rightarrow p\}$. We speak of an α- or ω-limit set L of v if there exists a streamline s in the vector field v that has L as α- or ω-limit set.*

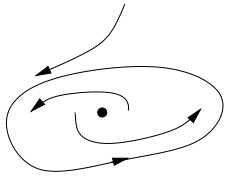

Fig. 1. Example for α- and ω-limit sets.

If the α- or ω-limit set of a streamline consists of only one point, this point is a critical point. The most common case of a α- or ω-limit set in a planar vector field containing more than one inner point of the domain is a closed streamline. Figure 1 shows an example for α- and ω-limit sets. There is one critical point and one closed streamline contained in the vector field. Both, the critical point and the closed streamline are their own α- and ω-limit set. For every other streamline the closed streamline is the ω-limit set. If the streamline starts inside the closed streamline, the critical point is the α-limit set. Otherwise the α-limit set is empty. With these explanations, we can give a precise definition of a topological feature of a vector field.

Definition 3.5 (Topological feature)
Let v be a vector field. Then, a ***topological feature*** *of v is an α- or ω-limit set of the vector field v describing the asymptotic behavior of the flow.*

As motivated in the previous example, sources, sinks, and most closed streamlines are considered such a topological feature.

4 Detection in Planar Flows

As can be seen from the definition of sinks and sources, these topological features are relatively easy to determine by calculating the eigenvalues of the flow. Unfortunately, it is not as easy to find the closed streamlines of a flow. Therefore, this chapter describes an algorithm that detects if an arbitrary streamline c converges to a closed curve, also called a limit cycle. This means that c has γ as α- or ω-limit set depending on the orientation of integration. We do not assume any knowledge on the existence or location of the closed curve. We exploit the fact that we use linear interpolation inside the cells for the proof of our algorithm. But the principle of the algorithm works on any piecewise defined planar vector field where one can determine the topology inside the pieces.

4.1 Detection of Closed Streamlines

In a precomputational step every singularity of the vector field is determined. To find all stable closed streamlines we mainly compute the topological skeleton of the vector field. We use an ordinary streamline integrator, such as an ODE solver using Runge-Kutta, as a basis for our algorithm. In addition, this streamline integrator is extended so that it is able to detect closed streamlines. In order to find all closed streamlines that reside inside another closed streamline we have to continue integration after we found a closed streamline inside that region.

The basic idea of our streamline integrator is to determine a region of the vector field that is never left by the streamline. According to the Poincaré-Bendixson-Theorem, a streamline approaches a closed streamline if no singularity exists in that region. To reduce computational cost we first integrate the streamline using a Runge-Kutta-method of fifth order with an adaptive stepsize control. Every cell that is crossed by the streamline is stored during the computation. If a streamline approaches a limit cycle it has to reenter the same cell again. This results in a *cell cycle*.

Definition 4.1 (Cell cycle)
Let s be a streamline in a given vector field v. Further, let G be a set of cells representing an arbitrary rectangular or triangular grid without any holes. Let $C \subset G$ be a finite sequence $c_0, \ldots, c_n$ of neighboring cells where each cell is crossed by the streamline s in exactly that order and $c_0 = c_n$. If s crosses every cell in C in this order again while continuing, C is called a ***cell cycle****.*

This cell cycle identifies the previously mentioned region. To check if this region can be left we could integrate backwards starting at every point on the boundary of the cell cycle. If there is one point converging to the currently investigated streamline we know for sure that the streamline will leave the cell cycle. If not, the currently investigated streamline will never leave the cell cycle. Since there are infinitely many points on the boundary this, of course, results in a non-terminating algorithm. To solve this problem we have to reduce the number of points that need to be checked. Therefore we define *potential exit points*:

Definition 4.2 (Potential exit points)
Let C be a cell cycle in a given grid G as in definition 4.1. Then there are two kinds of ***potential exit points****. First, every vertex of the cell cycle C is a* ***potential exit point****. Second, every point on an edge at the boundary of C where the vector field is tangential to the edge is also a* ***potential exit point****. Here, only edges that are part of the boundary of the cell cycle are considered. Additionally, only the* ***potential exit points*** *in the spiraling direction of the streamline need to be taken into account.*

To determine if the streamline leaves the cell cycle, a backward integrated streamline is started to see where a streamline has to enter the cell cycle in order to leave at that exit. We will show later that it is sufficient to only check these potential exit points to test if the streamline can leave the cell cycle.

Definition 4.3 (Real exit points)
Let P be a potential exit point of a given cell cycle C as in definition 4.2. If the backward integrated streamline starting at P does not leave the cell cycle after one full turn through the cell cycle, the potential exit point is called a ***real exit point****.*

Since a streamline cannot cross itself, the backward integration starting at a real exit point converges to the currently investigated streamline. Consequently, the currently investigated streamline leaves the cell cycle near that real exit point. Figure 2(a) shows an example for such a real exit point.

If on the other hand no real exit point exists we can determine for every potential exit point where there is a region with an inflow that leaves at that potential exit. Consequently, the currently investigated streamline cannot leave near that potential exit point as shown in figure 2(b).

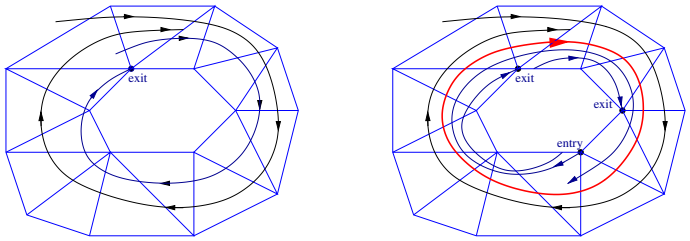

(a) (b)

Fig. 2. If a real exit point can be reached, the streamline will leave the cell cycle (a); if no real exit point can be reached, the streamline will approach a limit cycle (b).

With these definitions we can formulate the main theorem for the algorithm:

Theorem 4.4
Let C be a cell cycle with no singularity inside and E the set of potential exit points. If there is no real exit point among the potential exit points E or there are no potential exit points at all then there exists a closed streamline inside the cell cycle.

Proof: *(Sketch)*
Let C be the cell cycle. It is obvious that the streamline cannot leave the cell cycle C if all backward integrated streamlines started at every point on the boundary of C leave the cell cycle C. According to the Poincaré-Bendixson-theorem, there exists a closed streamline inside the cell cycle in that case.

We will show now that it is sufficient to only consider the potential exit points. If the backward integrated streamlines starting at all these potential exit points leave the cell cycle the backward integration of any point on an edge will also do.

Figure 3 shows the different configurations of potential exits. Let E be an arbitrary point on an edge between two potential exit points. In part *(a)* both

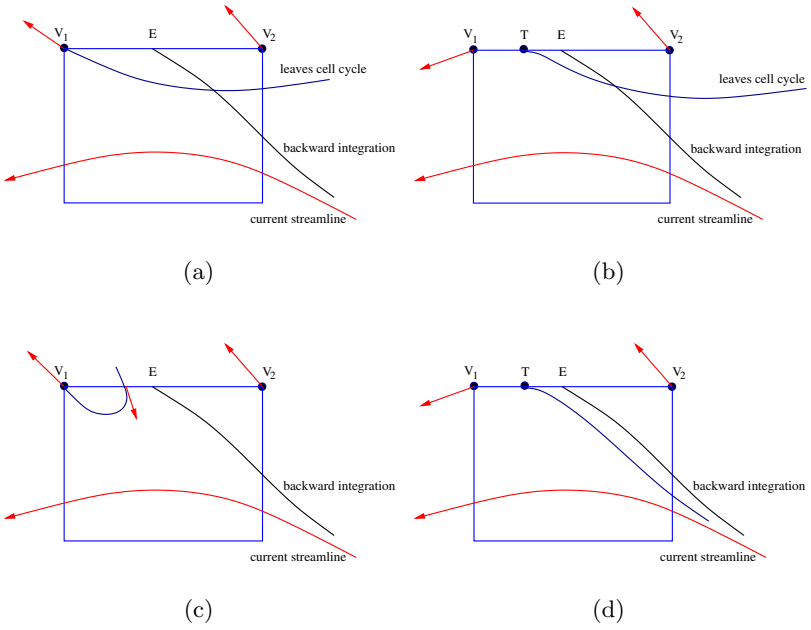

Fig. 3. Different cases of potential exits. (a) and (b) is impossible because streamlines cannot cross each other, (c) contradicts the linear interpolation on an edge, in (d) backward integrations converge to the current streamline so that the point E is a real exit.

backward integrated streamlines starting at the vertices V_1 and V_2 leave the cell cycle. Consequently, E cannot be an exit. It would need to cross one of the other backward integrated streamlines which is not possible.

Part *(b)* of figure 3 shows the case where the vector at a point on the edge is tangential to the edge. Obviously, if E lies between V_1 and T the backward integrated streamline will leave the cell cycle immediately. If it lies between T and V_2 and converges to the currently investigated streamline it has to cross the backward integrated streamline started at T. This contradicts the fact that streamlines cannot cross each other. Because of the linear interpolation at the edge, part *(c)* is also impossible.

We have shown that the currently investigated streamline cannot leave the cell cycle if there are only real exits. Consequently, there exists a closed streamline inside the cell cycle C since there is no singularity inside C. ❑

With theorem 4.4 it is possible to describe the algorithm in detail. It mainly consists of three different stages: first a streamline is integrated and one cell change after the other is identified. At each cell the algorithm checks if a cell cycle is completed. In case of a cell cycle it looks for exits by going backwards through the crossed cells and looking for potential exit points. Finally, the exits that were found are validated. Therefore, a streamline starting at the potential exit is integrated backwards through the whole cell cycle. If it is not possible to integrate backwards one full turn throughout the cell cycle for at least one backward integration a closed streamline resides in this cell cycle.

Otherwise the forward integration of the original streamline is continued. The algorithm exits if no real exit points are found among all of the potential exit points or if a critical point or the boundary of the vector field is reached. Theorem 4.4 guarantees that the algorithm then detects closed streamlines if every potential exit point [32] is checked.

5 Detection of Features in 3-D Vector Fields

Closed streamlines can be found in three-dimensional vector fields as well. For instance, the *Terrestrial Planet Finder Mission* of NASA [21] deals with stable manifolds where 3-D periodic halo orbits play an important role. These orbits are nothing else than closed streamlines in a three-dimensional vector field.

This section describes how to detect closed streamlines in three-dimensional vector fields. Although the principle to detect closed streamlines in a three-dimensional vector field is similar to the two-dimensional case, there are some differences. The following subsections explain the theoretical and algorithmic differences and similarities.

5.1 Theory

It is assumed that the data is given on a tetrahedral grid, but the principle would work on other cell types as well. The detection of a cell cycle works in the same way as in definition 4.1. Of course, the cells are three-dimensional in this case. To check if we can leave the cell cycle we have to consider every backward integrated streamline starting at an arbitrary point on a face of the boundary of the cell cycle. Looking at the edges of a face we can see directly that it is not sufficient to just integrate streamlines backwards. It is necessary to integrate a stream-surface backwards starting at an edge of the cell cycle. The streamlines starting at the vertices of that edge may leave the cell cycle earlier than the complete surface. In fact, it often occurs that one of these streamlines exit the cell cycle directly while parts of the stream surface itself may stay inside. Consequently, a different definition for exits is required.

Definition 5.1 (Potential Exit Edges)
Let C be a cell cycle in a given tetrahedral grid G as in Definition 4.1. Then we call every edge at the boundary of the cell cycle a ***potential exit edge****. Analogue to the two-dimensional case we define a line on a boundary face where the vector field is tangential to the face as a* ***potential exit edge*** *also.*

Due to the fact that we use linear interpolation inside the tetrahedrons it can be shown that there will be at least a straight line on the face where the vector field is tangential to the face or the whole face is tangential to the vector field [33]. Therefore, isolated points on a face where the vector field is tangential to the face do not need to be considered. When dealing with edges as exits, stream-surfaces need to be computed in order to validate these exits. Analogue to definition 4.3 we define *real exit edges*.

Definition 5.2 (Real exit edge)
Let E be a potential exit edge of a given cell cycle C as in definition 5.1. If the backward integrated stream-surface does not completely *leave the cell cycle after one full turn through C then this edge is called a* ***real exit edge****.*

For the backward integrated stream-surface a simplified version of the stream-surface algorithm introduced by Hultquist [16] is used. Since there is no triangulation of the surface required, only the integration step of that algorithm needs to be executed. Initially, we start the backward integration at the vertices of the edge. If the distance between two neighboring backward integrations is greater than a specific error limit a new backward integration is started in-between. This continues until an approximation of the stream-surface that respects the given error limit has been reached.

The integration stops when the whole stream-surface leaves the cell cycle or when one full turn through the cell cycle is completed. To construct the surface properly it may be necessary to continue a backward integration process across the boundary of the cell cycle. This is due to the fact that parts of the stream-surface are still inside the cell but the backward integrated streamlines have already left it. With these definitions and motivations we can formulate the main theorem for the algorithm:

Theorem 5.3
Let C be a cell cycle as in definition 4.1 with no singularities inside and E the set of potential exit edges. If there is no real exit edge among the potential exit edges E or there are no potential exit edges at all then there exists a closed streamline inside the cell cycle.

Proof: *(Sketch)*
Let C be a cell cycle with no real exit edge. Every backward integrated stream-surface leaves the cell cycle C completely. As in the 2-D case it is obvious that the cell cycle cannot be left if every backward integration starting at an arbitrary point on a face of the boundary of the cell cycle C leaves that cell cycle. Let Q be an arbitrary point on a face F of the boundary of the cell cycle C. Let us assume that the backward integrated streamline starting at Q converges to the currently investigated streamline. We will show that this is a contradiction.

First case: *The edges of face F are exit edges and there is no point on F where the vector field is tangential to F.*
From a topological point of view the stream-surfaces starting at all edges of F form a tube that leaves the cell cycle. Since the backward integrated streamline starting at Q converges to the currently investigated streamline it does not leave the cell cycle. Consequently, it has to cross the tube formed by the stream-surfaces. This is not possible because streamlines cannot cross each other and therefore a streamline cannot cross a stream-surface either.

Second case: *There is a potential exit edge e on the face F that is not part of the boundary of F.*
Obviously, the potential exit edge e divides the face F into two parts. In one part there is outflow out of the cell cycle

C while at the other part there is inflow into C because the flow is tangential at e. We do not need to consider the part with outflow any further because every backward integrated streamline starting at a point of that part immediately leaves the cell cycle C.
The backward integrated surface starting at the potential exit edge e and parts of the backward integrated stream-surfaces starting at the boundary edges of the face F again form a tube from a topological point of view. Consequently, the backward integrated streamline starting at Q has to leave the cell cycle C.

We have shown that the backward integrated streamline starting at the point Q has to leave the cell cycle also. Since there is no backward integrated streamline converging to the currently investigated streamline at all, the streamline will never leave the cell cycle. ❑

5.2 Algorithm

With theorem 5.3 it is possible to describe the algorithm in detail. Similar to the two-dimensional case, a streamline is integrated while every cell change is memorized to detect cell cycles. If a cell cycle was found the algorithm looks for potential exits by going backwards through the cell cycle and validating these using backward integrated stream-surfaces. According to theorem 5.3, there exists a closed streamline inside this cell cycle if all backward integrated stream-surfaces leave the cell cycle. In that case, we can find the exact location by continuing the integration process of the streamline that we currently investigate until the difference between two subsequent turns is small enough. This numerical criterion is sufficient in this case since the streamline will never leave the cell cycle.

6 Results

The first example is a simulation of a swirling jet with an inflow into a steady medium. The simulation originally resulted in a three-dimensional vector field but we used a cutting plane and projected the vectors onto this plane to get a two-dimensional field. In this application one is interested in investigating the turbulence of the vector field and in regions where the fluid stays for a very long time. This is necessary because some chemical reactions need a special amount of time. These regions can be located by finding closed streamlines. Figure 4 shows some of the closed streamlines detected by our algorithm in detail. In addition, a hedgehog representation of the vector field is given. All these limit cycles are located in the upper region of the vector field. Figure 5 shows all closed streamlines of this vector field including the topological skeleton.

To test our 3-D detection, a synthetically created dataset which includes one closed streamline is used. We first created a two-dimensional vector field.

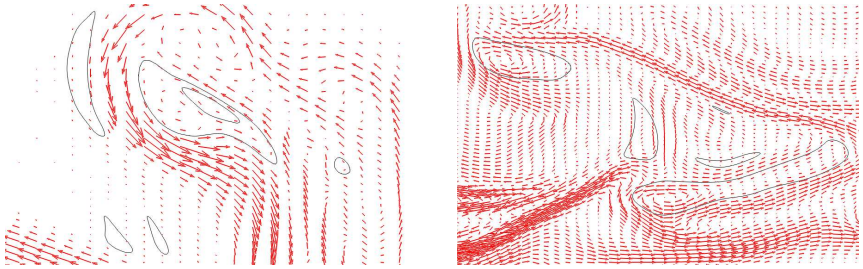

Fig. 4. Vorticity vector field of a turbulent flow – limit cycles.

The vector field contains a saddle singularity in the center and two symmetrical sinks. To get a three-dimensional flow we rotated the two-dimensional vector field around the axis of symmetry. Due to the symmetrical arrangement of the sinks this vector field includes exactly one closed streamline. Figure 6 shows the result of the algorithm including two stream-surfaces to depict the surrounding flow. Since the closed streamline is attracting, the stream-surfaces approaches the closed streamline. The stream-surface gets smaller and smaller while spiraling around the closed streamline. After a few turns around the closed streamline, it is only slightly wider than a streamline and finally it totally merges with the closed streamline. A random color scheme for the surface is used to enhance the three-dimensional effect. Overall, it is shown that the algorithms discussed in this paper are capable of detecting most of the previously defined features.

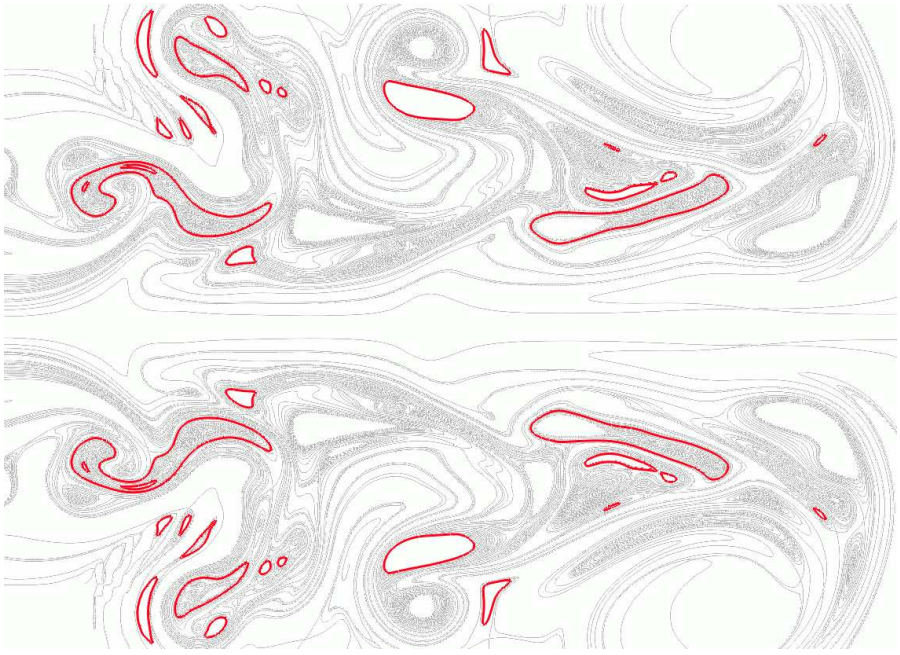

Fig. 5. Vorticity vector field visualized by the topological skeleton including closed streamlines.

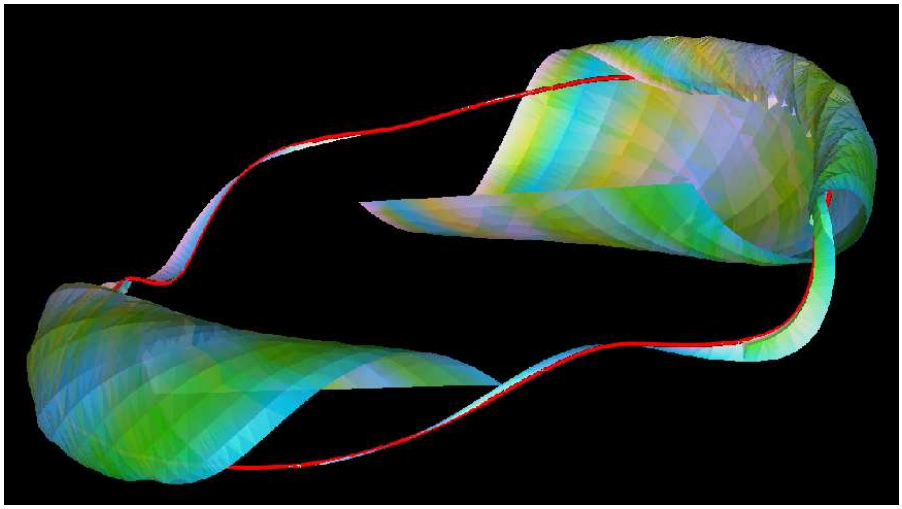

Fig. 6. Limit cycle in a 3-D vector field with stream-surfaces.

7 Impending Challenges

If more than one closed streamline crosses the same cell, the algorithm may fail to detect these closed streamlines, for instance, if there is a structural unstable configuration with one closed streamline inside the other both located in the same cell cycle. One closed streamline acts like a source, lets say the inner one, while the other one behaves like a sink. Therefore, the flow originates at the first one and is attracted by the second one. Since there is an outflow from the cell cycle the algorithm cannot distinguish between a regular outflow and this configuration. A solution for such a situation could be to use a subdivision of the grid for the detection of cell cycles only to avoid the presence of two closed streamlines in the same cell cycle. In addition, the algorithm for finding closed streamlines in 3-D needs to be applied to more realistic datasets. Also, there exist more closed structures in 3-D such as a torus for instance. Therefore, the algorithm could be extended to find these structures as well.

8 Conclusion

In order to complete the topological analysis of vector fields, this article defined topological features solely based on the asymptotic behavior of the flow. Since singularities are not the only features inside a vector field that can attract or repel the surrounding flow, this is an important extension to topological analyses. Algorithms were presented that are capable of successfully detecting these topological features both in two- and three-dimensional vector fields.

9 Acknowledgments

We would like to thank the graphics group at the University of Technology at Kaiserslautern, Germany, especially Hans Hagen, Gerik Scheuermann,

Xavier Tricoche, and all the students working in this group. Part of this work was funded by DFG (Deutsche Forschungsgemeinschaft) and Land Rheinland-Pfalz, Germany. Wolfgang Kollmann, Mechanical and Aeronautical Engineering Department of the University of California at Davis, provided us with the vorticity dataset. We are very grateful for this and several helpful hints and discussions.

References

1. R. H. Abraham and C. D. Shaw. *Dynamics – The Geometry of Behaviour: Bifurcation Behaviour*. Aerial Press, Inc., Santa Cruz, 1982.
2. T. J. Aprille and T. N. Trick. A computer algorithm to determine the steady-state response of nonlinear oscillators. *IEEE Transactions on Circuit Theory*, CT-19(4), July 1972.
3. D. Bürkle, M. Dellnitz, O. Junge, M. Rumpf, and M. Spielberg. Visualizing complicated dynamics. In A. Varshney, C. M. Wittenbrink, and H. Hagen, editors, *IEEE Visualization '99 Late Breaking Hot Topics*, pp. 33 – 36, San Francisco, 1999.
4. M. S. Chong, A. E. Perry, and B. J. Cantwell. A General Classification of Three-Dimensional Flow Fields. *Physics of Fluids*, A2(5), pp. 765–777, 1990.
5. U. Dallmann. Topological Structures of Three-Dimensional Flow Separations. Technical Report DFVLR-AVA Bericht Nr. 221-82 A 07, Deutsche Forschungs- und Versuchsanstalt für Luft- und Raumfahrt e.V., April 1983.
6. W. de Leeuw and R. van Liere. Collapsing flow topology using area metrics. In D. Ebert, M. Gross, and B. Hamann, editors, *IEEE Visualization '99*, pp. 349–354, San Francisco, 1999.
7. M. Dellnitz and O. Junge. On the Approximation of Complicated Dynamical Behavior. *SIAM Journal on Numerical Analysis*, 36(2), pp. 491 – 515, 1999.
8. G. Fischel, H. Doleisch, L. Mroz, H. Löffelmann, and E. Gröller. Case study: visualizing various properties of dynamical systems. In *Proceedings of the Sixth International Workshop on Digital Image Processing and Computer Graphics (SPIE DIP-97)*, pp. 146–154, Vienna, Austria, October 1997.
9. A. Globus, C. Levit, and T. Lasinski. A Tool for Visualizing the Topology of Three-Dimensional Vector Fields. In G. M. Nielson and L. Rosenblum, editors, *IEEE Visualization '91*, pp. 33 – 40, San Diego, 1991.
10. E. Gröller, H. Löffelmann, and R. Wegenkittl. Visualization of Analytically Defined Dynamical Systems. In *Proceedings of Dagstuhl '97*, pp. 71–82. IEEE Scientific Visualization, 1997.
11. J. Guckenheimer. Numerical analysis of dynamical systems, 2000.
12. J. L. Helman and L. Hesselink. Automated analysis of fluid flow topology. In *Three-Dimensional Visualization and Display Techniques, SPIE Proceedings Vol. 1083*, pp. 144–152, 1989.
13. J. L. Helman and L. Hesselink. Visualizing Vector Field Topology in Fluid Flows. *IEEE Computer Graphics and Applications*, 11(3), pp. 36–46, May 1991.
14. D. H. Hepting, G. Derks, D. Edoh, and R. D. Russel. Qualitative analysis of invariant tori in a dynamical system. In G. M. Nielson and D. Silver, editors, *IEEE Visualization '95*, pp. 342 – 345, Atlanta, GA, 1995.
15. M. W. Hirsch and S. Smale. *Differential Equations, Dynamical Systems and Linear Algebra*. Academic Press, New York, 1974.
16. J. P. M. Hultquist. Constructing Stream Surface in Steady 3D Vector Fields. In *Proceedings IEEE Visualization '92*, pp. 171–177. IEEE Computer Society Press, Los Alamitos CA, 1992.

17. A. Inselberg and B. Dimsdale. Parallel Coordinates: a Tool for Visualizing Multidimensional Geometry. In *IEEE Visualization '90 Proceedings*, pp. 361–378, Los Alamitos, 1990. IEEE Computer Society.
18. D. N. Kenwright. Automatic Detection of Open and Closed Separation and Attachment Lines. In D. Ebert, H. Rushmeier, and H. Hagen, editors, *IEEE Visualization '98*, pp. 151–158, Research Triangle Park, NC, 1998.
19. H. Löffelmann. *Visualizing Local Properties and Characteristic Structures of Dynamical Systems*. PhD thesis, Technische Universität Wien, 1998.
20. H. Löffelmann, T. Kučera, and E. Gröller. Visualizing Poincaré Maps Together with the Underlying Flow. In H.-C. Hege and K. Polthier, editors, *Mathematical Visualization, Algorithms, Applications, and Numerics*, pp. 315–328. Springer, 1997.
21. K. Museth, A. Barr, and M. W. Lo. Semi-Immersive Space Mission Design and Visualization: Case Study of the "Terrestrial Planet Finder" Mission. In *Proceedings IEEE Visualization 2001*, pp. 501–504. IEEE Computer Society Press, Los Alamitos CA, 2001.
22. A. E. Perry and B. D. Fairly. Critical Points in Flow Patterns. *Advances in Geophysics*, 18B, pp. 299–315, 1974.
23. R. Roussarie. *Bifurcations of Planar Vector Fields and Hilbert's Sixteenth Problem*. Birkhäuser, Basel, Switzerland, 1998.
24. G. Scheuermann, T. Bobach, H. Hagen, K. Mahrous, B. Hahmann, K. I. Joy, and W. Kollmann. A Tetrahedra-Based Stream Surface Algorithm. In *IEEE Visualization '01 Proceedings*, Los Alamitos, 2001. IEEE Computer Society.
25. G. Scheuermann, B. Hamann, K. I. Joy, and W. Kollmann. Visualizing local Vetor Field Topology. *Journal of Electronic Imaging*, 9(4), 2000.
26. X. Tricoche. *Vector and Tensor Field Topology Simplification, Tracking and Visualization*. PhD thesis, University of Kaiserslautern, 2002.
27. X. Tricoche, G. Scheuermann, and H. Hagen. Topology-Based Visualization of Time-Dependent 2D Vector Fields. In R. P. D. Ebert, J. M. Favre, editor, *Proceedings of the Joint Eurographics–IEEE TCVG Symposium on Visualization*, pp. 117–126, Ascona, Switzerland, 2001. Springer.
28. X. Tricoche, T. Wischgoll, G. Scheuermann, and H. Hagen. Topology Tracking for the Visualization of Time-Dependent Two-Dimensional Flows. *Computer & Graphics*, pp. 249–257, 2002.
29. M. van Veldhuizen. A New Algorithm for the Numerical Approximation of an Invariant Curve. *SIAM Journal on Scientific and Statistical Computing*, 8(6), pp. 951 – 962, 1987.
30. R. Wegenkittl, H. Löffelmann, and E. Gröller. Visualizing the Behavior of Higher Dimensional Dynamical Systems. In R. Yagel and H. Hagen, editors, *IEEE Visualization '97 Proceedings*, pp. 119 – 125, Phoenix, AZ, 1997.
31. T. Wischgoll. *Closed Streamlines in Flow Visualization*. PhD thesis, Universität Kaiserslautern, Germany, 2002.
32. T. Wischgoll and G. Scheuermann. Detection and Visualization of Closed Streamlines in Planar Flows. *IEEE Transactions on Visualization and Computer Graphics*, 7(2), 2001.
33. T. Wischgoll and G. Scheuermann. Locating Closed Streamlines in 3D Vector Fields. In *Joint Eurographics–IEEE TCVG Symposium on Data Visualization 2002*, pp. 227–232, Barcelona, Spain, 2002.
34. Y. Yan-qian, C. Sui-lin, C. Lan-sun, H. Ke-cheng, L. Ding-jun, M. Zhi-en, W. Ernian, W. Ming-shu, and Y. Xin-an. *Theory of Limit Cycles*. American Mathematical Society, Providence - Rhode Island, 1986.